Hindawi
Advances in Civil Engineering
Volume 2021, Article ID 3152619, 12 pages
https://doi.org/10.1155/2021/3152619

Research Article

Investigation on the Displacement Ductility Coefficient of Reinforced Concrete Columns Strengthened with Textile-Reinforced Concrete

Boxue Wang,[1] Shiping Yin ,[1,2] and Ming Liu[2]

[1]*State Key Laboratory for Geomechanics & Deep Underground Engineering, China University of Mining and Technology, Xuzhou 221116, China*
[2]*Jiangsu Key Laboratory of Environmental Impact and Structural Safety in Engineering, China University of Mining and Technology, Xuzhou 221116, China*

Correspondence should be addressed to Shiping Yin; ysp2010@cumt.edu.cn

Received 14 September 2021; Revised 11 November 2021; Accepted 23 November 2021; Published 7 December 2021

Academic Editor: Giulio Zani

To evaluate the seismic performance of reinforced concrete (RC) columns strengthened with textile-reinforced concrete (TRC), based on the ABAQUS numerical analysis results of 15 TRC-strengthened RC columns, the grey correlation theory was used to determine the input variables of the model, and the accuracy of the numerical simulation results is verified by some experiments. Then, according to FEM data, a neural network prediction model was established for the displacement ductility coefficients of TRC-strengthened columns, and a formula was proposed for calculating the displacement ductility coefficient. The results showed that the BP (backpropagation) neural network model had good rationality and accuracy and that the ductility coefficients of the strengthened columns calculated by the model agreed well with the experimental values. Therefore, the model can be applied for predicting the displacement ductility coefficients of TRC-strengthened columns and can be used as a reference for engineering design.

1. Introduction

Ductility is an important index for evaluating the seismic performance of concrete structures, and good ductility could avoid brittle failure of components and provide a certain safety reserve for components under accidental overload [1]. Reinforced concrete (RC) has been widely used in structural engineering applications all over the world [2], and as an important load-bearing component of structures, RC columns should provide sufficient strength, stiffness, and ductility so that the building can withstand earthquakes [3]. Therefore, studying the ductility of RC columns and evaluating their seismic performance are very important topics.

There are still a large number of buildings around the world that are not considered for seismic design and are likely to be affected by earthquakes [4–6]. To reduce the adverse effects of earthquakes on existing structures, several strengthening methods have been proposed and widely applied in practical projects over the past few decades. Because these traditional strengthening methods adopt concrete or steel [6, 7], these methods have shortcomings, such as increasing the structural weight, easily developing rust, and changing the structural appearance. In recent years, with the development of composite materials, fibre-reinforced polymers (FRPs), a new type of reinforcement material, have been used to strengthen and repair existing structures. To evaluate the seismic performance of strengthened structures, many scholars have conducted a series of studies [8–12]. The results in the literature show that FRPs can enhance the ductility and energy dissipation capacity of strengthened columns. Although FRPs have been widely used for effective reinforcement, FRPs are not suitable for use in humid environments because of their poor compatibility with concrete substrates and their lack of

vapour permeability due to the use of epoxy resin as an adhesive [13]. More importantly, it is difficult to examine and evaluate the status of the repaired structures, as the structures are obscured by the FRP reinforcement. To this end, Triantafillou et al. [13] introduced the concept of combining textile fibres with inorganic matrix (such as cement mortar). Due to the different matrix strengths and fibre types used by different scholars, this new type of cement-based material also has different names, such as textile-reinforced mortar (TRM) [13, 14], textile-reinforced concrete (TRC) [15], basalt-reinforced mortar (BRM) [16], and fabric-reinforced cementitious matrix (FRCM) [17]. The significant difference between FRP and cement-based matrix composites is the free edge stress concentration of FRP confinement, which will cause premature failure of the reinforcement system [18].

Bournas et al. [19, 20] studied the seismic performance of RC columns strengthened by TRM under earthquake action. Their results showed that TRM can improve the seismic performance and deformation capacity of strengthened columns. Yin et al. [21] explored the influence of different factors on the seismic performance of TRC-strengthened columns, and their results indicated that the ductility coefficient of strengthened columns increased with increasing reinforcement layers and stirrup ratio or decreasing axial compression ratio. Al-Salloum et al. [22] studied the effect of TRM on the shear strength and ductility of beam-column joints with deficient seismic performance. Their results showed that TRM can effectively improve the shear strength and ductility of beam-column joints with defects. In addition, the results in [23, 24] indicate that although the ductility coefficient of TRC-strengthened columns decreases to some extent under environmental erosion, the overall seismic performance of the strengthened columns is good.

Although TRC has received much attention in the field of seismic reinforcement, relatively few studies have focused on the ductility and deformation capacity of specimens after strengthening, and the relationships between various factors and the ductility coefficient have not been quantified. In addition, many problems in strengthening concrete column structures are nonlinear. The factors affecting the ductility of concrete columns are very complex, and there are certain coupling effects between the factors and the ductility of components. However, artificial neural networks have the ability to perform associative reasoning, simulation thinking, and self-adaptive recognition, which can be found in input-output mapping through learning [25, 26]. Therefore, artificial neural networks (ANN) are suitable for nonlinear reasoning and prediction in structural engineering. Back-propagation (BP) neural networks are the most widely used artificial neural networks, as BP neural networks have low requirements and limitations on known data and can make full use of existing data to analyze and study the evolution, development, and movement rules of objects [27, 28]. It has been successfully applied in civil engineering, such as design [29], prediction [30–33], optimization [34], and damage detection and identification [35, 36].

Therefore, based on the team's previous research results [37, 38], a BP neural network is applied to obtain the mapping relationship between ductility and various influencing factors of TRC-strengthened RC columns. Based on the mapping relationship, a ductility coefficient formula for reinforced columns is deduced, which enables accurate and efficient ductility calculations and provides a scientific basis for the evaluation of seismic performance of components and guidance for engineering design.

2. Grey Correlation Analysis

The grey system theory is based on the sequence operator to realize the law of things in the process of transformation. The original irregular data is generated into regular sequence, and then the differential equation method is used to predict and analyze the development trend of things objectively and scientifically. As the core content of grey system theory, grey correlation analysis is a method to predict the unknown information by using the known information. The grey correlation analysis is used to calculate the grey correlation degree of several factors. The larger the value of the correlation degree is, the greater the influence of the factor on the evaluation index is.

2.1. Significance of Grey Correlation Analysis. In this paper, grey system theory is applied to analyze the factors affecting the displacement ductility coefficient of TRC-strengthened columns, including the strength grade of existing concrete, axial compression ratio, shear span ratio, stirrup space, and number of textile layers. Finite element simulation results of TRC-strengthened columns were adopted as the sample data, and the following grey correlation analysis was carried out to obtain the ranking results of the correlation degree of various factors. The dominant factors affecting the displacement ductility coefficient of TRC-strengthened columns reflect the deformation capacity and seismic performance of TRC-strengthened columns to some extent. Therefore, the results of this study can also provide important references for future theoretical research and design applications of the displacement ductility coefficient of TRC-strengthened columns.

2.2. Correlation Analysis. In this paper, all the relevant correlation coefficients are gathered into one value, and the calculated average value is used to process the information. The correlation coefficient of each factor is calculated (i.e., the average value of all corresponding correlation coefficients), which is a quantitative analysis of the correlation degree between various factors and TRC-strengthened columns. The specific calculations and analyses are described hereafter.

2.2.1. Determination of Correlation Factors. According to the results of existing research, the main factors affecting the displacement ductility coefficient of strengthened RC columns are the strength grade of existing concrete, axial compression ratio, shear span ratio, stirrup space, and strengthening layers. The main content of this paper is to

determine the influence of strengthening layers, axial compression ratio, shear span ratio, and other parameters on the ductility coefficient. Therefore, the following correlation factors are selected as the comparison parameter sequence of the system: (1) reinforcement layers x_1 (0, 1, 2, 3, 4), (2) axial compression ratio x_2 (0.2, 0.3, 0.4, 0.5), (3) shear span ratio x_3 (2, 3.8, 5.6), (4) stirrup space x_4 (50 mm, 100 mm, 150 mm), and (5) concrete strength grade x_5 (C30, C40, C50, C60), namely, $\{x_i(k) \mid i = 1, 2, 3, 4, 5;\ k = 1, 2, 3, 4, 5\}$. The displacement ductility coefficient is obtained from 15 TRC-strengthened columns based on ABAQUS earthquake simulations in [37, 38] used as the generating sequence of the system. The specific geometric dimensions and reinforcing bars of the specimens are shown in Figure 1. And according to [37, 38], the numerical and experimental results match well (shown in Figure 2 [38]), which shows that the established model and the finite element analysis results are rational and accurate. The correlation factors and displacement ductility coefficient involved in the numerical analysis are shown in Table 1.

2.2.2. Dimensionless Data. The original data are initialized according to equation (1) [39], and the initialized data are shown in Table 2.

$$x_{i'}(k) = \frac{x_i(k)}{x_i(1)}, \quad i = 0, 1, 2, 3, 4, 5;\ k = 1, 2, \ldots, 15. \tag{1}$$

2.2.3. Calculation of Absolute Difference. According to equation (2), the absolute difference between the parent sequence and subsequence in Table 2 (i.e., the absolute difference value results for $\Delta_i(k)$) is shown in Table 3.

$$\Delta_i(k) = |x_{0'}(k) - x_{i'}(k)|, \quad i' = 1, 2, 3, 4, 5;\ k = 1, 2, \ldots, 15, \tag{2}$$

where $x_{0'}(k)$ is for the parent sequence (dimensionless) and $x_{i'}(k)$ is for the subsequence (dimensionless).

2.2.4. Calculation of the Correlation Coefficient. Equation (3) is used to calculate the correlation coefficient $\gamma_{0i}(k)$, and the results are shown in Table 4.

$$\gamma_{0i}(k) = \frac{m + ZM}{\Delta_i(k) + ZM}, \quad Z \in (0, 1), i = 1, 2, 3, 4, 5;\ k = 1, 2, 3, \ldots, 15, \tag{3}$$

where $\gamma_{0i}(k)$ is the correlation coefficient; Z is the resolution coefficient, which has a value that is generally between 0 and 1 and is typically taken as 0.5; m is the minimum second-order difference, which is 0 according to $m = \min_i \min_k \Delta i(k)$; and M is the maximum second-order difference, which is 3.02 according to $m = \max_i \max_k \Delta i(k)$.

2.2.5. Calculation of the Correlation Degree. The correlation degree between the subsequence x_i and the parent sequence x_0 is calculated according to equation (4), which is expressed as follows:

$$\gamma_i = \frac{1}{n} \sum_{k=1}^{n} \gamma_{0i}(k), n = 15, i = 1, 2, 3, 4, 5; k = 1, 2, 3, \ldots, 15. \tag{4}$$

The calculated correlation degree is $\gamma_i = \{0.59, 0.85, 0.88, 0.86, 0.86 \mid i = 1, 2, 3, 4, 5\}$.

2.2.6. Ranking of Correlation Degree. By sorting the correlation degree obtained from the calculation, the results show that the influence degree of each factor on the displacement ductility coefficient of TRC-strengthened columns is shear span ratio > (axial compression ratio, stirrup ratio, concrete strength) > TRC layers. In addition, combined with the value of the correlation degree, these five factors have a great impact on the ductility performance of TRC-strengthened columns. Therefore, based on these five factors, a BP neural network model was established by MATLAB to predict the ductility change trend of the TRC-strengthened columns.

3. Establishment of Neural Network Prediction Model

Based on MATLAB, the BP neural network model is established to predict the displacement ductility coefficient of TRC-strengthened columns. The specific operation steps are as follows.

3.1. BP Neural Network Construction. The structure of BP neural network mainly includes the number of neural network layers and neurons in each layer. Because the three-layer BP neural network has strong nonlinear mapping ability and can approach any nonlinear function, the three-layer BP neural network was used to model in this paper. The numbers of input layers, hidden layers, and output layers are all one. Based on the analysis mentioned above, BP neural network includes five input parameters, i.e., concrete strength grade, axial compression ratio, shear span ratio, stirrup space, and strengthening layers, and the output parameter is displacement ductility coefficient. The number of input layer and output layer neurons in the corresponding model is 5 and 1, respectively. The number of hidden layer neurons is determined by formula (5) [40] and multiple training calculations. The structure of BP neural network model is shown in Figure 3.

$$D = \sqrt{D_i + D_0} + a, \tag{5}$$

where D is the number of nodes in the hidden layer, D_i is the number of input nodes, D_0 is the number of output nodes, and a is between 1 and 10.

In addition, the essence of BP learning algorithm is to get the minimum value of error function. Because it uses the steepest descent method in nonlinear programming to

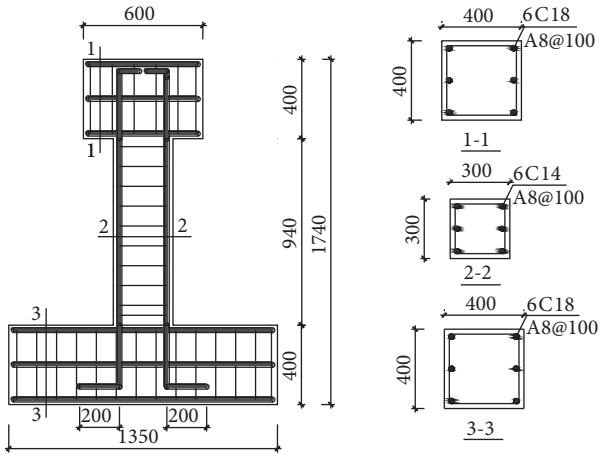

Figure 1: Specimen size and reinforcement details.

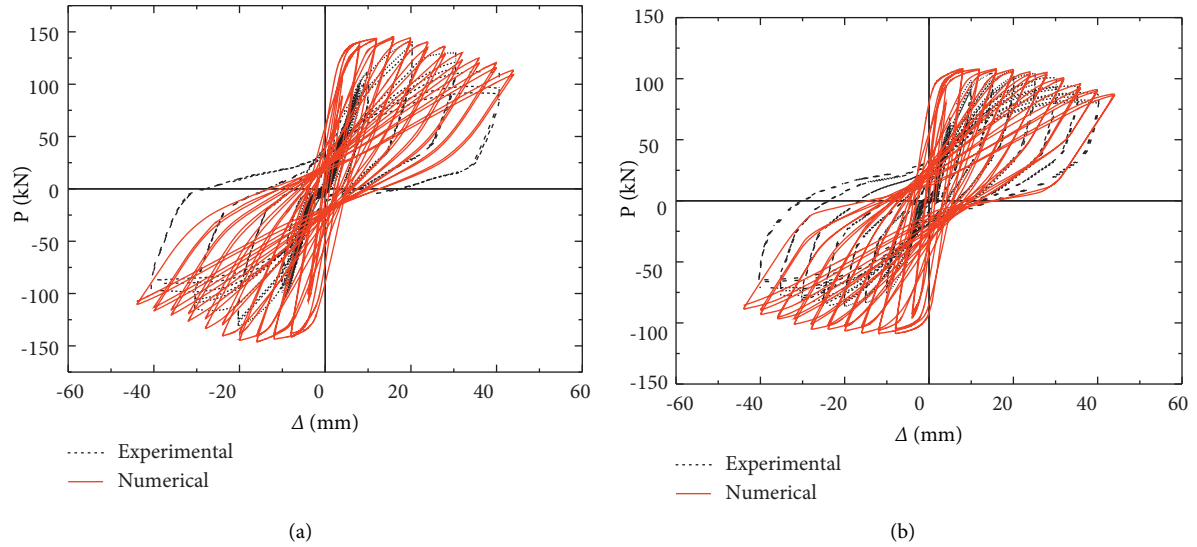

Figure 2: Hysteresis curves with different axial compression ratios of TRC-strengthened RC columns. (a) Axial compression ratios with 0.25. (b) Axial compression ratios with 0.15.

Table 1: Original data of the specimens.

Serial number	Ductility coefficient $x_0(k)$	Reinforcement layer $x_1(k)$	Axial compression ratio $x_2(k)$	Shear span ratio $x_3(k)$	Stirrup reinforcement ratio $x_4(k)$ (%)	Concrete strength grade $x_5(k)$
1	6.76	1	0.3	3.8	0.34	40
2	4.36	0	0.3	3.8	0.34	40
3	6.91	2	0.3	3.8	0.34	40
4	6.50	3	0.3	3.8	0.34	40
5	6.60	4	0.3	3.8	0.34	40
6	10.58	2	0.2	3.8	0.34	40
7	5.30	2	0.4	3.8	0.34	40
8	3.73	2	0.5	3.8	0.34	40
9	3.38	2	0.3	2.0	0.34	40
10	6.69	2	0.3	5.6	0.34	40
11	7.59	2	0.3	3.8	0.67	40
12	5.32	2	0.3	3.8	0.22	40
13	3.79	2	0.3	3.8	0.34	30
14	5.03	2	0.3	3.8	0.34	50
15	5.00	2	0.3	3.8	0.34	60

Table 2: Initialized data of the specimens.

Serial number	Ductility coefficient $x_{0'}(k)$	Reinforcement layer $x_{1'}(k)$	Axial compression ratio $x_{2'}(k)$	Shear span ratio $x_{3'}(k)$	Stirrup reinforcement ratio $x_{4'}(k)$	Concrete strength grade $x_{5'}(k)$
1	1.00	1.00	1.00	1.00	1.00	1.00
2	0.64	0.00	1.00	1.00	1.00	1.00
3	1.02	2.00	1.00	1.00	1.00	1.00
4	0.96	3.00	1.00	1.00	1.00	1.00
5	0.98	4.00	1.00	1.00	1.00	1.00
6	1.57	2.00	0.67	1.00	1.00	1.00
7	0.78	2.00	1.33	1.00	1.00	1.00
8	0.55	2.00	1.67	1.00	1.00	1.00
9	0.50	2.00	1.00	0.53	1.00	1.00
10	0.99	2.00	1.00	1.47	1.00	1.00
11	1.12	2.00	1.00	1.00	1.97	1.00
12	0.79	2.00	1.00	1.00	0.65	1.00
13	0.56	2.00	1.00	1.00	1.00	0.75
14	0.74	2.00	1.00	1.00	1.00	1.25
15	0.74	2.00	1.00	1.00	1.00	1.50

Table 3: Absolute difference of the specimens.

Serial number	Ductility coefficient $\Delta_0(k)$	Reinforcement layer $\Delta_1(k)$	Axial compression ratio $\Delta_2(k)$	Shear span ratio $\Delta_3(k)$	Stirrup reinforcement ratio $\Delta_4(k)$	Concrete strength grade $\Delta_5(k)$
1	1	0	0	0	0	0
2	0.64	0.64	0.36	0.36	0.36	0.36
3	1.02	0.98	0.02	0.02	0.02	0.02
4	0.96	2.04	0.04	0.04	0.04	0.04
5	0.98	3.02	0.02	0.02	0.02	0.02
6	1.57	0.43	0.9	0.57	0.57	0.57
7	0.78	1.22	0.55	0.22	0.22	0.22
8	0.55	1.45	1.12	0.45	0.45	0.45
9	0.5	1.5	0.5	0.03	0.5	0.5
10	0.99	1.01	0.01	0.48	0.01	0.01
11	1.12	0.88	0.12	0.12	0.85	0.12
12	0.79	1.21	0.21	0.21	0.14	0.21
13	0.56	1.44	0.44	0.44	0.44	0.19
14	0.74	1.26	0.26	0.26	0.26	0.51
15	0.74	1.26	0.26	0.26	0.26	0.76

Table 4: Correlation coefficient data of the specimens.

Serial number	$\gamma_{01}(k)$	$\gamma_{02}(k)$	$\gamma_{03}(k)$	$\gamma_{04}(k)$	$\gamma_{05}(k)$
1	1.00	1.00	1.00	1.00	1.00
2	0.70	0.81	0.81	0.81	0.81
3	0.61	0.99	0.99	0.99	0.99
4	0.43	0.97	0.97	0.97	0.97
5	0.33	0.99	0.99	0.99	0.99
6	0.78	0.63	0.73	0.73	0.73
7	0.55	0.73	0.87	0.87	0.87
8	0.51	0.57	0.77	0.77	0.77
9	0.50	0.75	0.98	0.75	0.75
10	0.60	0.99	0.76	0.99	0.99
11	0.63	0.93	0.93	0.64	0.93
12	0.56	0.88	0.88	0.92	0.88
13	0.51	0.77	0.77	0.77	0.89
14	0.55	0.85	0.85	0.85	0.75
15	0.55	0.85	0.85	0.85	0.67

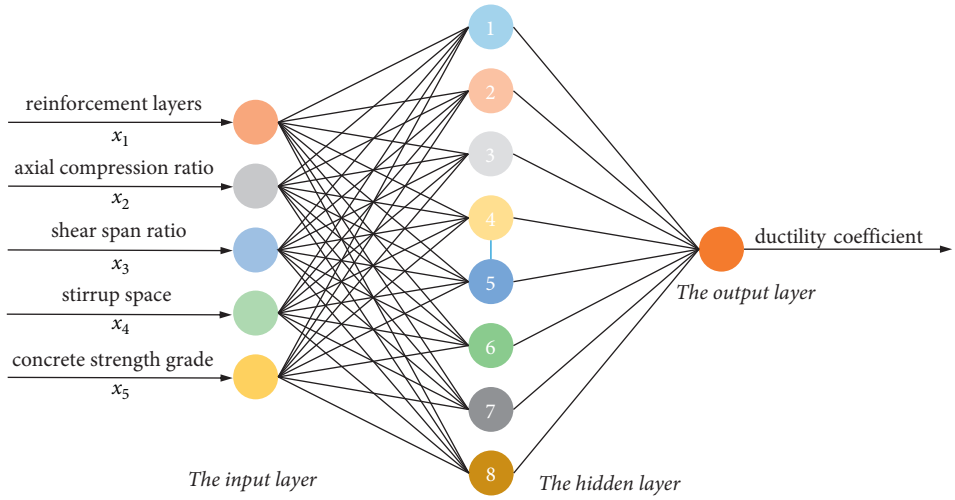

Figure 3: Architecture of three-layer backpropagation (BP) neural network model.

modify the weights according to the negative gradient direction of error function, it usually has shortcomings such as low learning efficiency, slow convergence speed, and easy fall into local minimum state. Several optimization techniques are proposed to speed up the convergence of the BP learning algorithm [41, 42]. The results indicate that the Levenberg-Marquardt (L-M) algorithm was very efficient when training networks. The flowchart of L-M algorithm is shown in Figure 4.

3.2. Determine Sample Data. A small number of experiments have been designed to prove the accuracy of the finite element results. After verification, the finite element simulation results are in good agreement with the test results, which proves that the finite element simulation results are accurate. In order to better perform parametric analysis, in this paper, the training sample data (10 groups) and test sample data (5 groups) for the model are determined according to the data obtained from simulation calculations. Moreover, considering the calculation efficiency and error of the model, all the sample data are normalized according to equation (6) before the sample is input into the model. The relevant linear transformation algorithm is expressed as follows:

$$y = \frac{(x - \min)}{(\max - \min)}, \tag{6}$$

where x is the input vector, min is the minimum value of x, max is the maximum value of x, and y is the output vector.

At the same time, the parameter ε_i (weight coefficient) is introduced to obtain the true correlation between the influencing factors and TRC-strengthened columns, and the specific formula is shown in equation (7). The weight coefficient is combined with the data in Table 5 to obtain the input data for the final model. The specific results are shown in Table 6.

$$\varepsilon_i = \frac{\gamma_i}{\sum_{k=1}^{5} \gamma_{0i}}, \quad i = (1, 2, 3, 4, 5), \tag{7}$$

where γ_i is the correlation value between each factor and displacement ductility coefficient calculated in Section 1 and Section 2 of this paper.

In this paper, the five associated values $\gamma_i = \{0.59, 0.85, 0.88, 0.86, 0.86 \mid k = 1, 2, 3, 4, 5\}$ obtained in the previous section are substituted into (7), and the weight coefficients of each factor are obtained as follows: 0.146, 0.210, 0.218, 0.213, and 0.213. Then, the weight coefficients are multiplied by the normalized data to obtain the input data. The detailed results are shown in Table 6.

3.3. Simulation of the Neural Network. The sample data obtained above (shown in Table 6) were input into the established and trained neural network model, and the accuracy of the model was verified by comparing and analyzing the results of the neural network model and the simulated calculation.

3.4. Neural Network Predicted Value. Table 7 and Figure 5 show a comparison between the predicted value of the displacement ductility coefficient calculated by the BP neural network model and the displacement ductility coefficient of the TRC reinforced column obtained by finite element analysis in previous studies.

In addition, data analysis software, Statistical Product and Service Solutions (SPSS) [43], was used to compare the predicted value of displacement ductility coefficient calculated in the above BP neural network model with the experimental value obtained by numerical analysis, and the correlation between the value predicted by the BP neural network and the experimental value was obtained. The specific parameters are shown in Table 8.

Table 8 shows that the R^2 of the fitting degree between the predicted value of displacement ductility coefficient calculated based on the BP neural network model and the measured value calculated by the above simulation is 0.83. Therefore, the results show that the BP neural network model based on the grey correlation analysis method has a

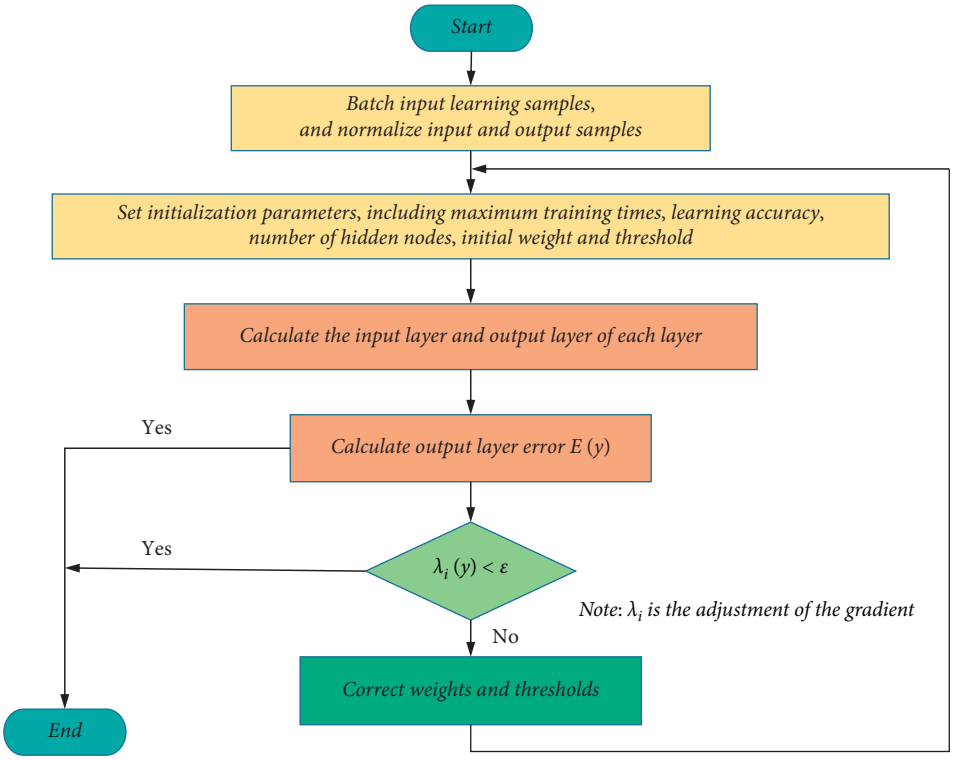

Figure 4: A flowchart of Levenberg-Marquardt algorithm.

Table 5: Normalized data of the specimens.

Serial number	Reinforcement layer	Axial compression ratio	Shear span ratio	Stirrup reinforcement ratio	Concrete strength grade
1	0.00	0.33	0.50	0.27	0.33
2	0.25	0.33	0.50	0.27	0.33
3	0.50	0.33	0.50	0.27	0.33
4	0.75	0.33	0.50	0.27	0.33
5	1.00	0.33	0.50	0.27	0.33
6	0.50	0.00	0.50	0.27	0.33
7	0.50	0.67	0.50	0.27	0.33
8	0.50	1.00	0.50	0.27	0.33
9	0.50	0.33	0.00	0.27	0.33
10	0.50	0.33	1.00	0.27	0.33
11	0.50	0.33	0.50	1.00	0.33
12	0.50	0.33	0.50	0.00	0.33
13	0.50	0.33	0.50	0.27	0.00
14	0.50	0.33	0.50	0.27	0.67
15	0.50	0.33	0.50	0.27	1.00

good prediction effect on the displacement ductility coefficient of TRC-strengthened RC columns.

4. Ductility Formula

The displacement ductility coefficient reflects the plastic deformation capacity of the structural member. It is the ratio of the failure displacement of the specimen to the yield displacement, namely,

$$\mu = \frac{\Delta_u}{\Delta_y}, \tag{8}$$

where Δ_u is the ultimate displacement of the specimen, which is the horizontal displacement when the horizontal load drops to 85% of the peak load; Δ_y is the yield displacement of the specimen, which is the corresponding horizontal displacement when the specimen reaches the initial yield point.

According to the correlation analysis and grey correlation analysis of the factors influencing the seismic performance of TRC-strengthened RC column mentioned in Section 1 and Section 2, the displacement ductility coefficient of the TRC-strengthened RC column changes with changes in the shear span ratio, axial compression ratio, stirrup space, and concrete strength grade and TRC layers.

Table 6: Sample input sample data.

Serial number	Reinforcement layer	Axial compression ratio	Shear span ratio	Stirrup reinforcement ratio	Concrete strength grade
1	0.00	0.07	0.11	0.06	0.07
2	0.04	0.07	0.11	0.06	0.07
3	0.07	0.07	0.11	0.06	0.07
4	0.11	0.07	0.11	0.06	0.07
5	0.15	0.07	0.11	0.06	0.07
6	0.07	0.00	0.11	0.06	0.07
7	0.07	0.14	0.11	0.06	0.07
8	0.07	0.21	0.11	0.06	0.07
9	0.07	0.07	0.00	0.06	0.07
10	0.07	0.07	0.22	0.06	0.07
11	0.07	0.07	0.11	0.21	0.07
12	0.07	0.07	0.11	0.00	0.07
13	0.07	0.07	0.11	0.06	0.00
14	0.07	0.07	0.11	0.06	0.14
15	0.07	0.07	0.11	0.06	0.21

Table 7: Comparison of measured and predicted values.

Serial number	Displacement ductility coefficient		
	Measured value	Predicted value	Measured/predicted value
1	4.36	4.52	0.964
2	6.76	5.91	1.144
3	6.91	6.42	1.076
4	6.5	6.40	1.016
5	6.6	6.49	1.016
6	10.58	10.62	0.996
7	5.3	5.23	1.014
8	3.73	5.69	0.656
9	3.38	3.39	0.998
10	6.69	6.77	0.989
11	7.59	7.56	1.004
12	5.32	5.27	1.009
13	3.79	5.74	0.661
14	5.03	5.12	0.982
15	5	4.99	1.002

Therefore, the influences of the shear span ratio, axial compression ratio, stirrup space, and concrete strength grade are considered when deducing the displacement ductility coefficient of the reinforced column.

In this section, the influence of the shear span ratio, axial compression ratio, stirrup ratio, fibre braided mesh layout layers, concrete strength grade, and TRC layers on the displacement ductility coefficient of TRC-strengthened RC columns is considered to establish a function according to [44]. The function form is expressed in the following equation:

$$\mu = \frac{a + c(\lambda - d)\sqrt{\lambda_v} + e\lambda_s/(g + \lambda)}{\text{in} + j}, \tag{9}$$

where μ is the displacement ductility coefficient, λ_s is the characteristic value of the fibre volume, and λ is the shear span ratio. The *a, c, d, e, g, i, j* are regression coefficients to be determined.

The characteristic values of stirrup volume and fibre volume can be calculated according to equations (10) and (11), respectively:

$$\lambda_v = \rho_v \frac{f_{yv}}{f_c} = \frac{nA_s l}{A_{\text{cor}} s} \frac{f_{yv}}{f_c} = \frac{A_{sv} l_g}{l_1 l_2 s_g} \times \frac{f_{yv}}{f_c}, \tag{10}$$

$$\lambda_s = \rho_s \frac{f_s}{f_c} = \frac{\tau_s l_s}{bh} \times \frac{f_{su}}{f_c}, \tag{11}$$

where λ_v is the characteristic value of the stirrup volume; f_c is the compressive strength of the concrete; ρ_v is the volume matching rate; n is the axial compression ratio; s the sectional area of tensile steel bars; l is the length of the stirrup; A_{cor} is the concrete core area; A_s is the stirrup space; f_{yv} is the stirrup design strength; A_{sv} is the cross-sectional area of stirrup; l_g is the perimeter of the stirrups; l_1 and l_2 are the lengths of two sides of the rectangular stirrups; s_g is the stirrup spacing; λ_s is the characteristic value of the fibre volume; τ_s and l_s are the section thickness and total perimeter of the carbon fibres, respectively; b and h are the cross-sectional width and height of the column; and f_{su} is the ultimate tensile strength of the carbon fibres.

Relevant parameters of TRC-strengthened columns that consider the shear span ratio, axial compression ratio, stirrup ratio, TRC layers, and concrete strength grade in Table 9 and

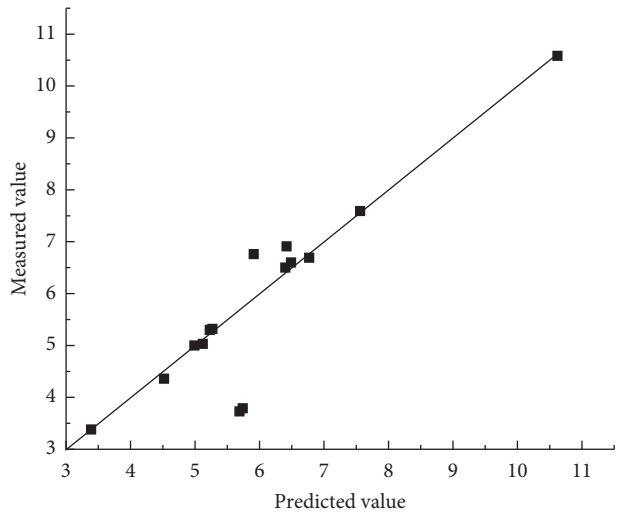

Figure 5: Ratio of measured value and predicted value of displacement ductility coefficient (Table 7).

Table 8: BP neural network predicted value fit.

Model	R	R^2	Adjusted R^2	Standard deviation error
1	0.911	0.830	0.817	0.696

Table 9: Raw sample data.

Serial number	Ductility coefficient μ	Reinforcement layer λ_s	Axial compression ratio n	Shear span ratio λ	Stirrup reinforcement ratio λ_v	Concrete strength grade
1	4.36	0.00	0.3	3.8	0.037	40
2	6.76	0.08	0.3	3.8	0.037	40
3	6.91	0.15	0.3	3.8	0.037	40
4	6.50	0.23	0.3	3.8	0.037	40
5	6.60	0.30	0.3	3.8	0.037	40
6	10.58	0.15	0.2	3.8	0.037	40
7	5.30	0.15	0.4	3.8	0.037	40
8	3.73	0.15	0.5	3.8	0.037	40
9	3.38	0.15	0.3	2.0	0.037	40
10	6.69	0.15	0.3	5.6	0.037	40
11	7.59	0.15	0.3	3.8	0.074	40
12	5.32	0.15	0.3	3.8	0.024	40
13	3.79	0.20	0.3	3.8	0.050	30
14	5.03	0.12	0.3	3.8	0.031	50
15	5.00	0.10	0.3	3.8	0.026	60

the displacement ductility coefficient obtained by numerical calculation are used as the input sample (ten sets of sample data and five sets of test data). Then, the data are substituted into MATLAB software for nonlinear regression to obtain the value of the regression coefficient. Then the regression coefficient is substituted into equation (9) to obtain equation (12). The results of the calculation and analysis are compared as shown in Table 10.

$$\mu = \frac{0.66 + 1.24(\lambda - 1.49)\sqrt{\lambda_v} + 3.16\lambda_s/(0.65 + \lambda)}{n - 0.07}. \quad (12)$$

A further comparison between the calculated and experimental displacement ductility coefficient was performed with the data analysis software SPSS, and the predictive value fit of the proposed formula was assessed, as shown in Table 10 and Figure 6. Table 11 shows that the R^2 is 0.805, the adjusted R^2 value after considering the number of independent variables is 0.790, and most of the errors between the predicted and simulated values calculated by the formula are within 15%. Therefore, the calculated and experimental results are in good agreement, indicating that the proposed equation can provide a reference for engineering design and seismic performance evaluation.

Table 10: Comparison of the measured and predicted value.

Serial number	Displacement ductility coefficient		
	Measured value	Predicted value	Measured/predicted value
1	4.36	5.27	0.83
2	6.76	5.51	1.23
3	6.91	5.73	1.21
4	6.5	5.98	1.09
5	6.6	6.19	1.07
6	10.58	10.13	1.04
7	5.3	3.99	1.33
8	3.73	3.06	1.22
9	3.38	4.18	0.81
10	6.69	7.46	0.90
11	7.59	6.72	1.13
12	5.32	5.26	1.01
13	5.64	6.27	0.90
14	5.03	5.43	0.93
15	5	5.19	0.96

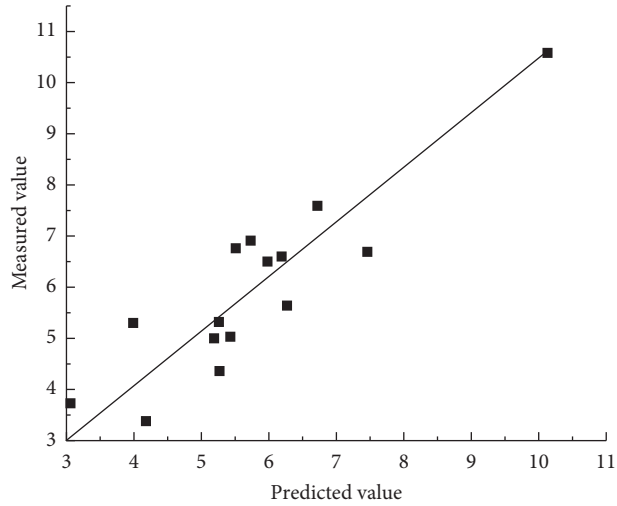

Figure 6: Ratio of measured value and predicted value of displacement ductility coefficient (Table 10).

Table 11: Predicted value fit of the proposed formula.

Model	R	R^2	Adjusted R^2	Standard deviation error
1	0.897	0.805	0.790	0.810

5. Conclusions

Based on the numerical analysis results, the correlation degree between the TRC layers, axial compression ratio, shear span ratio, stirrup space, concrete strength grade, and ductility of TRC-strengthened columns was analyzed. Furthermore, a BP neural network prediction model based on grey system theory was established in MATLAB, and then a formula was proposed for the displacement ductility coefficient of TRC-strengthened columns. The specific conclusions of this study are as follows:

(1) The influence of various factors on the ductility coefficient of reinforced columns is ranked as follows: shear span ratio > (axial compression ratio, stirrup space, and concrete strength grade) > TRC layers. This ranking was obtained by calculating the correlation value between the displacement ductility coefficient and various factors of TRC-strengthened columns. These results indicate that the factors selected in this paper have a substantial impact on the ductility of reinforced columns, and the correlations of these factors are strong.

(2) A BP neural network model with three layers was established to predict the displacement ductility coefficient of TRC-strengthened columns. The results show that the model can be used to predict the ductility coefficient of TRC-strengthened columns.

(3) Based on the developed BP neural network prediction model, which is based on grey system theory, a formula for calculating the displacement ductility coefficients of TRC-strengthened columns is

established by considering the influences of the shear span ratio, axial compression ratio, stirrup space, textile layers, and concrete strength grade on the displacement ductility coefficient. A verification process with relevant data shows that the calculated values are in good agreement with the experimental values, which indicates that the proposed ductility formula has a certain accuracy and rationality and that the formula can be used for predicting displacement ductility coefficients of TRC-strengthened columns and can provide a certain reference for engineering design.

Data Availability

The datasets used or analyzed during the current study are available from the corresponding author on reasonable request.

Conflicts of Interest

The authors declare that there are no conflicts of interest regarding the publication of this paper.

Acknowledgments

The authors gratefully acknowledge the financial support from the Program of the National Natural Science Foundation of China (Grant no. 51478458). The experimental work described in this paper was conducted at the Jiangsu Key Laboratory of Environmental Impact and Structural Safety in Civil Engineering in the China University of Mining and Technology. The support during the testing from staffs and students at the Laboratory is greatly acknowledged.

References

[1] S. S. Zheng, H. J. Lou, X. F. Wang, and Z. Li, "Study on displacement ductility coefficient of steel reinforced high-strength concrete column," *Advanced Materials Research*, vol. 368-373, pp. 1097–1100, 2012.

[2] B.-T. Huang, Q.-H. Li, S.-L. Xu, and B. Zhou, "Strengthening of reinforced concrete structure using sprayable fiber-reinforced cementitious composites with high ductility," *Composite Structures*, vol. 220, pp. 940–952, 2019.

[3] H. F. Ghatte, M. Comert, C. Demir, and A. Ilki, "Seismic retrofit of full-scale substandard extended rectangular RC columns through CFRP Jacketing: test results and design recommendations," *Journal of Composites for Construction*, vol. 23, no. 1, pp. 04018071~1–17, 2019.

[4] Y. A. Al-Salloum and T. H. Almusallam, "Seismic response of interior RC beam-column joints upgraded with FRP sheets. I: experimental study," *Journal of Composites for Construction*, vol. 11, no. 6, pp. 575–589, 2007.

[5] M. A. Zanini, L. Hofer, F. Faleschini, P. Zampieri, N. Fabris, and C. Pellegrino, "Preliminary macroseismic survey of the 2016 Amatrice seismic sequence," *Ann. Geophys.-Italy*, vol. 59, pp. 1–6, 2016, FastTrack5.

[6] F. Faleschini, J. Gonzalez-Libreros, M. A. Zanini, L. Hofer, L. Sneed, and C. Pellegrino, "Repair of severely-damaged RC exterior beam-column joints with FRP and FRCM composites," *Composite Structures*, vol. 207, pp. 352–363, 2019.

[7] A. Ghobarah and T. El-Amoury, "Seismic rehabilitation of deficient exterior concrete frame joints," *Journal of Composites for Construction*, vol. 9, no. 5, pp. 408–416, 2005.

[8] C. Yalcin, O. Kaya, and M. Sinangil, "Seismic retrofitting of R/C columns having plain rebars using CFRP sheets for improved strength and ductility," *Construction and Building Materials*, vol. 22, no. 3, pp. 295–307, 2008.

[9] A. Ilki, C. Demir, I. Bedirhanoglu, and N. Kumbasar, "Seismic retrofit of brittle and low strength RC columns using fiber reinforced polymer and cementitious composites," *Advances in Structural Engineering*, vol. 12, no. 3, pp. 325–347, 2009.

[10] O. Ozcan, B. Binici, and G. Ozcebe, "Seismic strengthening of rectangular reinforced concrete columns using fiber reinforced polymers," *Engineering Structures*, vol. 32, no. 4, pp. 964–973, 2010.

[11] C. Jiang, Y.-F. Wu, and G. Wu, "Plastic hinge length of FRP-confined square RC columns," *Journal of Composites for Construction*, vol. 18, no. 4, pp. 04014003–4014011~12, 2014.

[12] H. Farrokh Ghatte, M. Comert, C. Demir, and A. Ilki, "Evaluation of FRP confinement models for substandard rectangular RC columns based on full-scale reversed cyclic lateral loading tests in strong and weak directions," *Polymers*, vol. 8, no. 9, pp. 323–331~24, 2016.

[13] T. C. Triantafillou, C. G. Papanicolaou, P. Zissimopoulos, and T. Laourdekis, "Concrete confinement with textile-reinforced mortar jackets," *ACI Structural Journal*, vol. 103, no. 1, pp. 28–37, 2006.

[14] L. Koutas, A. Pitytzogia, T. C. Triantafillou, and S. N. Bousias, "Strengthening of infilled reinforced concrete frames with TRM: study on the development and testing of textile-based anchors," *Journal of Composites for Construction*, vol. 18, no. 3, pp. 40130155–A4013021~12, 2014.

[15] R. Ortlepp and S. Ortlepp, "Textile reinforced concrete for strengthening of RC columns: a contribution to resource conservation through the preservation of structures," *Construction and Building Materials*, vol. 132, pp. 150–160, 2017.

[16] M. Di Ludovico, A. Prota, and G. Manfredi, "Structural upgrade using basalt fibers for concrete confinement," *Journal of Composites for Construction*, vol. 14, no. 5, pp. 541–552, 2010.

[17] L. Ombres and S. Verre, "Structural behaviour of fabric reinforced cementitious matrix (FRCM) strengthened concrete columns under eccentric loading," *Composites Part B: Engineering*, vol. 75, pp. 235–249, 2015.

[18] A. Zinno, G. P. Lignola, A. Prota, G. Manfredi, and E. Cosenza, "Influence of free edge stress concentration on effectiveness of FRP confinement," *Composites Part B: Engineering*, vol. 41, pp. 523–532, 2010.

[19] D. A. Bournas, T. C. Triantafillou, K. Zygouris, and F. Stavropoulos, "Textile-reinforced mortar versus FRP jacketing in seismic retrofitting of RC columns with continuous or lap-spliced deformed bars," *Journal of Composites for Construction*, vol. 13, no. 5, pp. 360–371, 2009.

[20] D. A. Bournas and T. C. Triantafillou, "Bar buckling in RC columns confined with composite materials," *Journal of Composites for Construction*, vol. 15, no. 3, pp. 393–403, 2011.

[21] S. P. Yin, Y. Li, Y. Yang, and T. Ye, "Influencing factors of seismic performance of RC columns strengthened with textile reinforced concrete," *Journal of Zhejiang University (Engineering Science)*, vol. 51, no. 5, pp. 904–913, 2017, in Chinese.

[22] Y. A. Al-Salloum, N. A. Siddiqui, H. M. Elsanadedy, A. A. Abadel, and M. A. Aqel, "Textile-reinforced mortar

versus FRP as strengthening material for seismically deficient RC beam-column joints," *Journal of Composites for Construction*, vol. 15, no. 6, pp. 920–933, 2011.

[23] S. P. Yin, Y. Yang, T. Ye, and Y. Li, "Experimental research on seismic behavior of reinforced concrete columns strengthened with TRC under corrosion environment," *Journal of Structural Engineering*, vol. 143, no. 5, pp. 04016231–1~11, 2017.

[24] Y. Li, S. P. Yin, and W. J. Chen, "Seismic behavior of corrosion-damaged RC columns strengthened with TRC under a chloride environment," *Construction and Building Materials*, vol. 201, pp. 736–745, 2019.

[25] Q. H. Feng and W. C. Yuan, "Comparative study on BP neural network and RBF neural network in performance evaluation of seismic resistance for pier columns," *Structural Engineers*, vol. 23, no. 5, pp. 41–47+69, 2007, in Chinese.

[26] H. X. Fu and H. Zhao, *MATLAB Neural Network Application Design*, China Mechine Press, Beijing, China, 2010.

[27] K. B. Kim, K. B. Sim, and S. H. Ahn, "Recognition of concrete surface cracks using the ART1-based RBF network," *Lecture Notes in Computer Science*, no. 3972, pp. 669–6751, 2006.

[28] Q. H. Feng and W. C. Yuan, "A method based on RBFNN to predict the shear strength of steel reinforced high-strength concrete columns," *Structural Engineers*, vol. 24, no. 3, pp. 60–65, 2008, in Chinese.

[29] S. Wang, G. Sun, W. Chen, and Y. Zhong, "Database self-expansion based on artificial neural network: an approach in aircraft design," *Aerospace Science and Technology*, vol. 72, pp. 77–83, 2018.

[30] S. Tohidi and Y. Sharifi, "Neural networks for inelastic distortional buckling capacity assessment of steel I-beams," *Thin-Walled Structures*, vol. 94, pp. 359–371, 2015.

[31] I. M. Nikbin, S. Rahimi, and H. Allahyari, "A new empirical formula for prediction of fracture energy of concrete based on the artificial neural network," *Engineering Fracture Mechanics*, vol. 186, pp. 466–482, 2017.

[32] Ł. Sadowski, M. Piechówka-Mielnik, T. Widziszowski, A. Gardynik, and S. Mackiewicz, "Hybrid ultrasonic-neural prediction of the compressive strength of environmentally friendly concrete screeds with high volume of waste quartz mineral dust," *Journal of Cleaner Production*, vol. 212, pp. 727–740, 2019.

[33] V. L. Tran, D. K. Thai, and S. E. Kim, "Application of ANN in predicting ACC of SCFST column," *Composite Structures*, vol. 228, Article ID 111332, 2019.

[34] T. Y. Liu, P. Zhang, Y. F. Wang, and Y. F. Ling, "Compressive strength prediction of PVA fiber-reinforced cementitious composites containing Nano-SiO2 using BP neural network," *Materials*, vol. 13, p. 521, 2020.

[35] C. S. N. Pathirage, J. Li, L. Li, H. Hao, W. Q. Liu, and P. H. Ni, "Structural damage identification based on autoencoder neural networks and deep learning," *Engineering Structures*, vol. 172, pp. 13–28, 2018.

[36] Z. Tan, D. Thambiratnam, T. Chan, T. H. T. Chan, and H. A. Razak, "Detecting damage in steel beams using modal strain energy based damage index and artificial neural network," *Engineering Failure Analysis*, vol. 79, pp. 253–262, 2017.

[37] M. Liu, S. P. Yin, and W. J. Chen, "Seismic behaviour of TRC-strengthened RC columns under different constraint conditions," *Science and Engineering of Composite Materials*, vol. 26, no. 1, pp. 360–378, 2019.

[38] Y. Li, S. P. Yin, J. Y. Dai, and M. Liu, "Numerical investigation on the influences of different factors on the seismic performance of TRC - strengthened RC columns," *Journal of Building Engineering*, vol. 30, pp. 101245–101251~11, 2020.

[39] W. L. Pan, *Application of Grey System Theory in Security Engineering and Research on Aided Software*, Dalian Jiaotong University, Dalian, China, 2018.

[40] G. Mirchandani and W. Cao, "On hidden nodes for neural nets," *IEEE Transactions on Circuits and Systems*, vol. 36, no. 5, pp. 661–664, 2002.

[41] I. N. Daliakopoulos, P. Coulibaly, and I. K. Tsanis, "Groundwater level forecasting using artificial neural networks," *Journal of Hydrology*, vol. 309, pp. 229–240, 2005.

[42] H. Naderpour, O. Poursaeidi, and M. Ahmadi, "Shear resistance prediction of concrete beams reinforced by FRP bars using artificial neural networks," *Measurement*, vol. 126, pp. 299–308, 2018.

[43] J. L. Lu, X. M. Wang, H. Wang, Z. M. Hong, and Y. Y. Shan, "Applying of SPSS software in the teaching of mathematical statistics," in *Proceedings of the International Conference on Future Computer Supported Education (ICFCSE 2011)*, pp. 584–587, PEOPLES R CHINA, Chongqing, China, September 2011.

[44] W. H. Yu, *Study on Ductility Performance of Reinforced High concrete Columns Confined by CFRP*, Dalian University of Technology, Dalian, China, 2010, in Chinese.